This is a repository copy of *The application of plastic flow theory to inelastic column buckling*.

White Rose Research Online URL for this paper:
http://eprints.whiterose.ac.uk/98705/

Version: Accepted Version

1   **THE APPLICATION OF PLASTIC FLOW THEORY TO INELASTIC**

2   **COLUMN BUCKLING**

3   by Jurgen Becque[1]

4

5   **ABSTRACT**

6

7   The paper presents a theory of inelastic column buckling which is consistent with the

8   principles of plastic flow theory. The theory accounts for flexural, torsional and flexural-

9   torsional modes. While the use of the tangent modulus to describe inelastic flexural

10   buckling has been common place for a long time, efforts to comprehensively unite the

11   torsional and flexural-torsional modes with the principles of plastic flow theory have so far

12   been hampered by the 'plastic buckling paradox'. New theoretical developments presented

13   in this paper provide a way to achieve this goal. The solution hinges on the derivation of the

14   inelastic shear stiffness while considering an infinitesimal solid element embedded within

15   the column at a stage immediately past the point of buckling.

16   The proposed inelastic column theory is verified against selected experimental data

17   pertaining to aluminium and stainless steel columns of various cross-sections. Particular

18   attention is paid to the torsional buckling problem of the inelastic cruciform section column.

19

20   [1]Lecturer, Department of Civil and Structural Engineering, University of Sheffield, Sir

21   Frederick Mappin Building, Mappin Street, S1 3JD Sheffield, UK. Tel: +44 (0)114

22   2220252, J.Becque@Sheffield.ac.uk

1 **1. BACKGROUND**

2

3   With respect to inelastic flexural buckling of columns, Engesser (1889) was the first to

4   propose the use of the tangent modulus E_t to predict the buckling load of an initially

5   perfectly straight, inelastic column by modifying Euler's differential equation as follows:

6

7     $$E_t I \frac{d^2 u}{dx^2} + Pu = 0 \tag{1}$$

8

9   where u is the lateral column deflection, P is the axial compressive load and I is the second

10   moment of area of the cross-section about the principal axis about which bending takes

11   place. Eq. (1) results in an expression for the column buckling load:

12

13     $$P_{cr} = \pi^2 \frac{E_t I}{L_e^2} \tag{2}$$

14

15   where L_e is the effective length, dependent on the boundary conditions.

16   While straightforward, Engesser's approach received criticism from Considère (1891) who

17   argued that, as the column starts to bend out laterally, elastic unloading takes place on the

18   convex side of bending and that consequently, the bending stiffness is not simply

19   determined by $E_t I$. Engesser (1895) replied by proposing his "double-modulus" or "reduced

20   modulus" theory, where:

1    $$P_{cr} = \pi^2 \frac{E_r I}{L_e^2} \qquad (3)$$

2   with:

3    $$E_r = E_t \frac{I_c}{I} + E_0 \frac{I_t}{I} \qquad (4)$$

4   I_c and I_t are the second moments of area of the parts of the cross-section subjected to

5   compression and tension with respect to the neutral axis, respectively, and E_0 is the initial

6   elastic modulus.

7   It soon became apparent that Eq. (2) showed much better agreement with the experiment

8   than Eq. (3), which consistently led to overestimates. Shanley (1947) shed light on this

9   seeming paradox by pointing out that Eq. (2) does indeed constitute the buckling load of

10   the column since it indicates the point of bifurcation above which the column cannot be in a

11   state of stable equilibrium while remaining straight. Moreover, lateral buckling does not

12   take place under a constant load, but elastic unloading on the convex side instead results in

13   postbuckling capacity.

14   A realistic theory describing buckling of inelastic columns involving torsion, which may

15   either occur as pure torsional buckling or combined flexural and torsional buckling, based

16   on the principles of plastic flow theory has not yet been presented. The challenge thereby

17   lies in modelling the relationship between increments of shear stress and shear strain at the

18   onset of buckling. A previous interpretation of plastic flow theory (Hutchinson 1974,

19   Lubliner 1990, Bazant and Cedolin 1991) has suggested that the increments of shear stress

1   and shear strain remain linked through the elastic modulus E_0 at the onset of buckling and

2   that, therefore, the torsional resistance remains unaffected by the axially induced plasticity.

3   This conclusion, however, stands in clear contradiction with experimental observations, as

4   demonstrated by, among others, Batdorf (1949), Onat and Drucker (1952), Hutchinson

5   (1974), Lubliner (1990) and Bazant and Cedolin (1991). This "plastic buckling paradox",

6   as it is often named in literature, is particularly exemplified by the torsional buckling

7   problem of the inelastic cruciform column, since this particular cross-section relies on the

8   shear stresses resulting from pure torsion to a much larger extent than on the (negligible)

9   longitudinal warping stresses in its buckling resistance. Experiments on cruciform sections

10   have indicated that plastic flow theory substantially overestimates the buckling load. On the

11   other hand, buckling theories based on plastic deformation theory, which is generally

12   considered flawed and inferior in its concept to plastic flow theory, have so far yielded the

13   better predictions in relation to column buckling problems involving torsion. This is more

14   generally true for inelastic bifurcation problems and this paradoxical issue continues to

15   hamper theoretical stability research, as demonstrated recently by, for instance, Rønning et

16   al. (2010) for plates, Shamass et al. (2015) for cylindrical shells and Ruocco (2015) for

17   instabilities in thin-walled elements in general. The plastic buckling paradox has also been

18   excellently illustrated for thick and thin plates under uniaxial, biaxial and shear loading by

19   Wang et al. (2001), Wang and Tun Myint Aung (2007) and Wang and Huang (2009). The

20   problem also arises within the context of Generalized Beam Theory (GBT), as

21   demonstrated by Gonçalves and Camotim (2007). The authors developed two GBT

22   formulations, incorporating either deformation theory or flow theory. These new

4

1   formulations were then applied to the cases of simple plates under uniform compression

2   and hat section beams in uniform bending. It was concluded that the flow-based GBT

3   resulted in much higher predictions of the buckling stresses than the deformation-based

4   theory.

5   Interestingly, it has been observed (Shamass 2015) that the results of geometrically non-

6   linear finite element analyses using flow theory with an associated flow rule are unaffected

7   by the plastic buckling paradox. While no explanation has yet been provided as to why an

8   incremental numerical approach remedies the problem, a firm conclusion can be drawn

9   from this observation, namely that the plastic buckling paradox is not due to any inherent

10   shortcomings or limitations of flow theory itself, but rather a result of an incorrect

11   application of its principles. This idea is central to the theory proposed in this paper.

12   Onat and Drucker (1953) demonstrated that the plastic buckling paradox can be

13   circumvented by incorporating imperfections into the model and that even very small,

14   inevitable imperfections have a severe impact on the buckling load, reducing it to levels

15   close to those predicted by deformation theory. Hutchinson and Budiansky (1976)

16   confirmed this finding for low strain-hardening metals. However, they also demonstrated

17   that for metals with significant strain-hardening the imperfections have to be of such

18   magnitude that they can no longer be considered 'small and inevitable', thus suggesting that

19   Onat and Drucker's explanation is not entirely satisfying.

20   The approach presented in this paper differs from the aforementioned rationale in that a

21   perfectly straight column is considered, without initial imperfections. Instead, the plastic

22   buckling paradox is resolved by deriving a relationship between shear stress and shear

1   strain increments at the onset of buckling, while applying the plastic flow rule to a solid

2   element in its shear deformed shape. The basic principles of plastic flow theory, however,

3   are retained.

4

5   **2. INELASTIC SHEAR STIFFNESS**

6

7   An expression for the inelastic shear stiffness G_1 of a non-linear metal is first derived,

8   accounting for the presence of a uniaxial compressive stress. G_1 will be used in the

9   following paragraphs to relate increments of shear stress and shear strain at the point of

10   column buckling. The derivation here presented is a generalized and amended version of

11   the one contained in Becque (2010).

12   We consider the material stress-strain curve of a non-linear metal, as determined from a

13   uniaxial compression test (Fig. 1). It is a generally accepted postulate of plasticity that an

14   increment in axial strain $\dot{\varepsilon}_1$ is composed of an reversible elastic component $\dot{\varepsilon}_{1,el}$ and an

15   irreversible plastic component $\dot{\varepsilon}_{1,p}$:

16

17    $\dot{\varepsilon}_1 = \dot{\varepsilon}_{1,el} + \dot{\varepsilon}_{1,p}$ (5)

18

19   Eq. (5) can be written in terms of the increment in axial stress $\dot{\sigma}_1$ associated with $\dot{\varepsilon}_1$:

20

21    $\dfrac{\dot{\sigma}_1}{E_t} = \dfrac{\dot{\sigma}_1}{E_0} + \dfrac{\dot{\sigma}_1}{E_p}$ (6)

1

2   where E_0 is the elastic modulus, E_t is the tangent modulus at the relevant stress level and E_p

3   relates the plastic stress and strain increments. Thus:

4

5    $$\frac{1}{E_p} = \frac{1}{E_t} - \frac{1}{E_0} \qquad\qquad (7)$$

6

7   Plastic flow theory also dictates that the incremental plastic strain in the perpendicular

8   principal 2-direction is given by:

9

10    $$\dot{\varepsilon}_{2,P} = \kappa \dot{\varepsilon}_{1,P} \qquad\qquad (8)$$

11

12   An associated flow rule is adopted, so that κ in Eq. (8) is determined by the slope of the

13   normal to the flow surface (Drucker 1950). When the von Mises surface is used (Fig. 2), κ

14   amounts to -1/2 under uniaxial compression. However, the calculations will carry a general

15   κ value to allow for possible plastic anisotropy in the material.

16   Figure 3a depicts an infinitesimal element of material embedded within the column wall at

17   a certain depth in the thickness direction. Up to the point of buckling, the principal 1-

18   direction of stress coincides with the longitudinal axis of the column, while we orient the 2-

19   direction in the tangential direction along the heart line of the cross-section. When the

20   axially applied stress reaches a critical stress σ_{cr} with respect to the torsional or flexural-

21   torsional buckling mode, a further stress increment $\dot{\sigma}_1$ will cause the infinitesimal element

1   to undergo incremental deformations in the 1- and 2-directions, as well as deformations in

2   shear characterized by the angles $\dot{\theta}_1$ and $\dot{\theta}_2$ in Figure 3a. The angles $\dot{\theta}_1$ and $\dot{\theta}_2$ are, in

3   general, different as the infinitesimal element may also undergo a rigid body rotation

4   relative to the direction of the axial stress in addition to its shear deformations. The load on

5   the column is thereby assumed to be a gravity load or similar to a gravity load in a sense

6   that it maintains its vertical direction in space as the column buckles.

7   It is noted that the classical formulation of flow theory does not predict any plastic shear

8   deformations to take place in this process (Hutchinson 1974, Lubliner 1990, Bazant and

9   Cedolin 1991). In other words, the incremental shear deformations are purely elastic.

10   However, this point of view can be dislodged by considering the infinitesimal plate element

11   in its deformed shape (Figure 3a) in combination with Mohr's circle of the *incremental*

12   *plastic* strains (Figure 3b). For completeness, a few notes should be added. First, the

13   incremental plastic deformation in the thickness direction, $\dot{\varepsilon}_{3,p}$, is non-zero. However, since

14   the 3-direction constitutes a principal direction and is also the axis of rotation of our

15   reference system, the use of Mohr's circle is indeed justified. Second, plastic flow theory

16   dictates that the principal directions of the incremental plastic strains coincide with the

17   principal directions of the (total) stresses. At the point of buckling, infinitesimal plate

18   bending stresses and shear stresses develop. However, since these additional stresses are

19   initially infinitesimal, they do not affect the principal directions of stress. For the purpose of

20   considering the incremental step in Figure 3 immediately past the point of buckling, the

21   principal directions of stress (and thus of incremental plastic strain) remain firmly pointed

22   along the column axis and in the perpendicular direction within the column wall.

1   While the infinitesimal plate element in Figure 3a deforms, the sides a-a and b-b rotate

2   from their initial vertical and horizontal positions to final inclined positions at the end of

3   the load increment. At any stage during this transition, Mohr's circle indicates the

4   magnitude of plastic shearing which occurs along a-a and b-b. It is clear that, while planes

5   a-a and b-b rotate, the instantaneous magnitudes of the shear strains along a-a and b-b

6   (which are initially zero) gradually increase. The total plastic strain increments need

7   therefore be found by incremental integration, where the total increment in principal plastic

8   strain $\dot{\varepsilon}_{1,p}$ is subdivided into a number of intervals $\left(\dot{\varepsilon}_{1,p}/\dot{\theta}_1\right)d\alpha$. The sum of the $d\alpha$'s

9   thereby adds up to $\dot{\theta}_1$. In each interval the radius of Mohr's circle is given by:

10

11   $$R = \frac{(1-\kappa)}{2}\frac{\dot{\varepsilon}_{1,p}}{\dot{\theta}_1}d\alpha \qquad (9)$$

12

13   Therefore, the total plastic shear strains along a-a and b-b at the end of the increment are

14   found as follows:

15

16   $$\dot{\varepsilon}_{a,p} = \int\limits_{\alpha=0}^{\alpha=\dot{\theta}_1}\frac{(1-\kappa)}{2}\frac{\dot{\varepsilon}_{1,p}}{\dot{\theta}_1}\sin2\alpha \ d\alpha = -\frac{1}{2}\frac{(1-\kappa)}{2}\frac{\dot{\varepsilon}_{1,p}}{\dot{\theta}_1}\left(\cos2\dot{\theta}_1 - 1\right) \approx \frac{(1-\kappa)}{2}\dot{\theta}_1\dot{\varepsilon}_{1,p} \qquad (10)$$

17   $$\dot{\varepsilon}_{b,p} = -\int\limits_{\alpha=0}^{\alpha=\dot{\theta}_2}\frac{(1-\kappa)}{2}\frac{\dot{\varepsilon}_{1,p}}{\dot{\theta}_2}\sin2\alpha \ d\alpha = \frac{1}{2}\frac{(1-\kappa)}{2}\frac{\dot{\varepsilon}_{1,p}}{\dot{\theta}_2}\left(\cos2\dot{\theta}_2 - 1\right) \approx -\frac{(1-\kappa)}{2}\dot{\theta}_2\dot{\varepsilon}_{1,p} \qquad (11)$$

18

1   Eqs. (10-11) use the fact that, since Fig. 3a represents a state immediately past the point of

2   buckling, the angles $\dot{\theta}_1$ and $\dot{\theta}_2$ are necessarily small.

3   The increment in axial stress $\dot{\sigma}_1$ causes incremental shear stresses along the sides a-a and

4   b-b which, given the state of plane stress, can be determined using Mohr's circle for the

5   incremental stresses (Fig. 3c):

6

7    $$\dot{\tau}_a = \frac{\dot{\sigma}_1}{2} \sin 2\dot{\theta}_1 \approx \dot{\sigma}_1 \dot{\theta}_1 \qquad (12)$$

8    $$\dot{\tau}_b = -\frac{\dot{\sigma}_1}{2} \sin 2\dot{\theta}_2 \approx -\dot{\sigma}_1 \dot{\theta}_2 \qquad (13)$$

9   When a stress increment $\dot{\sigma}_1$ is applied in the axial direction of the column, the material

10   responds with a tangent stiffness E_t which is dependent on the stress level σ_1 and which can

11   be determined from the uniaxial stress-strain curve. At the point of buckling the strain

12   hardening rule can therefore be written (with the help of Eq. 7) as:

13

14   $$\dot{\varepsilon}_{1,p} = \frac{\dot{\sigma}_1}{E_p} = \dot{\sigma}_1 \left[\frac{1}{E_t} - \frac{1}{E_0} \right] \qquad (14)$$

15

16   Using Eq. (14) the angles $\dot{\theta}_1$ and $\dot{\theta}_2$ can be eliminated from Eqs. (9-10) and Eqs. (12-13):

17

18   $$\dot{\varepsilon}_{a,p} = \frac{(1-\kappa)}{2E_p} \dot{\tau}_a \qquad (15)$$

1     $\dot{\varepsilon}_{b,p} = \dfrac{(1-\kappa)}{2E_p}\dot{\tau}_b$ (16)

2

3   The constitutive equations (15-16) are independent of the angles $\dot{\theta}_1$ and $\dot{\theta}_2$ (within small

4   perturbations of the unbuckled state) and, by consequence, have to hold true at the point of

5   buckling itself. At this limit point, when the column is in an undeformed state (apart from

6   an axial shortening), the angles $\dot{\theta}_1$ and $\dot{\theta}_2$ are zero and the planes a-a and b-b in Fig. 3 are

7   perpendicular to each other. However, Eqs. (15-16) are still valid. In this undeformed state,

8   reciprocity of the shear stresses holds, and thus: $\dot{\tau}_a = \dot{\tau}_b = \dot{\tau}$, while the total plastic shear

9   straining can determined by adding Eqs. (15-16) (something which is, of course, not

10   possible in the deformed state):

11

12     $\dot{\gamma}_p = \dot{\varepsilon}_{a.p} + \dot{\varepsilon}_{b.p} = \dfrac{(1-\kappa)}{E_p}\dot{\tau}$ (17)

13

14   The elastic shear strain is governed by the well-known equation:

15

16     $\dot{\gamma}_{el} = \dfrac{\dot{\tau}}{G_0}$ (18)

17

18   where G_0 is the elastic shear modulus: $G_0 = E_0/[2(1+\nu)]$.

19   The total shear strain increment is then given by:

1

2 $$\dot{\gamma} = \dot{\gamma}_{el} + \dot{\gamma}_p = \left(\frac{1}{G_0} + \frac{1-\kappa}{E_p} \right) \dot{\tau} \qquad (19)$$

3

4 Using Eq. (7) to eliminate E_p yields the equation:

5

6 $$\dot{\tau} = \frac{E_t E_0}{(1+\kappa+2\nu)E_t + (1-\kappa)E_0} \dot{\gamma} \qquad (20)$$

7

8 The inelastic shear modulus G_1, valid at the point of buckling, is thus given by:

9

10 $$G_1 = \frac{E_t E_0}{(1+\kappa+2\nu)E_t + (1-\kappa)E_0} \qquad (21)$$

11

12 **3. DIFFERENTIAL EQUATIONS**

13

14 The differential equations describing the stability of an *elastic* thin-walled column without

15 imperfections have been presented by Timoshenko (1945) (*see also* Timoshenko and Gere

16 1961), based on earlier work by Kappus (1937), Wagner and Pretschner (1936), Bleich and

17 Bleich (1936), and Goodier (1942):

18

19 $$M_x = E_0 I_x \frac{d^2v}{dz^2} = -P(v - x_0\phi) \qquad (22)$$

1      $M_y = E_0 I_y \dfrac{d^2 u}{dz^2} = -P(u + y_0 \phi)$ (23)

2      $E_0 C_\omega \dfrac{d^4 \phi}{dz^4} - \left(G_0 J - \dfrac{I_p}{A} P\right)\dfrac{d^2 \phi}{dz^2} - Px_0 \dfrac{d^2 v}{dz^2} + Py_0 \dfrac{d^2 u}{dz^2} = 0$ (24)

3

4   In the above equations, the z-axis has been chosen to coincide with the longitudinal axis of

5   the column, while the x- and y-axes are the principal axes within the cross-section (Fig. 4).

6   The displacements u and v are those of the shear centre in the x- and y-directions,

7   respectively, while the angle ϕ measures the rotation of the cross-section about the

8   longitudinal axis through the shear centre. Furthermore, x_0 and y_0 are the coordinates of the

9   shear centre relative to the centroid C, P is the axial load, I_x and I_y are the second moments

10   of area about the x- and y-axes, respectively, C_ω is the warping constant, J is the torsional

11   constant, A is the cross-sectional area, and I_p is the polar moment of area:

12

13      $I_P = I_x + I_y + A\left(x_0^2 + y_0^2\right)$ (25)

14

15   When considering bifurcation of an *inelastic* column, the torsional resistance associated

16   with pure St. Venant torsion is governed by shear stresses which are linked to the shear

17   strains by the inelastic modulus G_1, as determined by Eq. (21). Therefore, the torsional

18   rigidity $G_0 J$ in Eq. (24) needs to be replaced by $G_1 J$ for an inelastic column. A second

19   contribution to the torsional resistance results from the development of longitudinal

20   warping stresses in non-uniform torsion. In an inelastic material, the longitudinal stress and

1   strain increments at the onset of buckling are related through the tangent modulus E_t.

2   Therefore, the warping resistance of an inelastic column at the onset of buckling is

3   governed by $E_t C_\omega$.

4   Furthermore, at the buckling load the longitudinal stress and strain increments due to

5   bending are also linked by the tangent modulus E_t. Shanley's insights (1947) thereby

6   indicate that no elastic unloading on the convex side of bending must be considered.

7   Based on these considerations, the differential equations describing stability of an inelastic

8   column can now be written as:

9

10
$$E_t I_x \frac{d^2 v}{dz^2} + P(v - x_0 \phi) = 0 \tag{26}$$

11
$$E_t I_y \frac{d^2 u}{dz^2} + P(u + y_0 \phi) = 0 \tag{27}$$

12
$$E_t C_\omega \frac{d^4 \phi}{dz^4} - \left(G_1 J - \frac{I_p}{A} P \right) \frac{d^2 \phi}{dz^2} - P x_0 \frac{d^2 v}{dz^2} + P y_0 \frac{d^2 u}{dz^2} = 0 \tag{28}$$

13

14   **3. COLUMNS WITH A DOUBLY SYMMETRIC CROSS-SECTION**

15   For columns with a doubly symmetric cross-section, the centroid and the shear centre

16   coincide, so that: $x_0 = y_0 = 0$, and: $I_p = I_x + I_y$. Eqs. (26-28) now become a set of uncoupled

17   differential equations:

18

19
$$E_t I_x \frac{d^2 v}{dz^2} + Pv = 0 \tag{29}$$

1     $E_t I_y \dfrac{d^2 u}{dz^2} + Pu = 0$ (30)

2     $E_t C_\omega \dfrac{d^4 \phi}{dz^4} - \left(G_1 J - \dfrac{I_p}{A} P \right) \dfrac{d^2 \phi}{dz^2} = 0$ (31)

3

4   For a pin-ended column where the end sections are free to warp, but prevented from

5   rotating about the longitudinal column axis, the boundary conditions are:

6

7     $u = v = \phi = 0$ for $z = 0, \ z = L$

8

9     $\dfrac{d^2 u}{dz^2} = \dfrac{d^2 v}{dz^2} = \dfrac{d^2 \phi}{dz^2} = 0$ for $z = 0, \ z = L$ (32)

10

11   Adopting the boundary conditions (32), the solution of Eqs. (26-28) is (*see* Timoshenko

12   and Gere 1961):

13

14     $P_x = \pi^2 \dfrac{E_t I_x}{L^2}$ (33)

15

16     $P_y = \pi^2 \dfrac{E_t I_y}{L^2}$ (34)

17

$$P_\phi = \frac{A}{I_p}\left(G_1 J + E_t C_\omega \frac{\pi^2}{L^2}\right) \tag{35}$$

3.1 Flexural Buckling

Eqs. (33) and (34), of course, do not represent new findings. Originally proposed by Engesser (1889), the use of the tangent modulus to determine the pure flexural buckling load of columns is widely used and accepted. Although elastic unloading at the convex side of bending results in post-buckling capacity (Shanley 1947), this post-buckling capacity is usually marginal for non-linear metals as a result of the rapid loss of stiffness at higher strain levels. Consequently, the tangent modulus approach has been demonstrated to yield good predictions of the ultimate capacity of columns failing in flexural buckling. Research confirming this finding has been carried out by, among others, Osgood and Holt (1938), Leary and Holt (1946), Holt and Leary (1946), Johnson and Winter (1966), Rasmussen and Hancock (1993) and van den Berg (2000). The aforementioned research includes test on various aluminium and stainless steel alloys and encompasses columns of various cross-sections.

Heimerl and Roy (1945) conducted tests on extruded 75S-T aluminium "thin-strip" columns with rectangular cross-section. These particular tests are here used to illustrate Eq. (34). Figure 5 compares the reported data to Eq. (34), where a Ramberg-Osgood representation (Ramberg and Osgood 1943) of the stress-strain curve was used to calculate the tangent modulus:

16

1

$$E_t = \frac{\sigma_{0.2\%} E_0}{\sigma_{0.2\%} + 0.002 n E_0 \left(\dfrac{\sigma}{\sigma_{0.2\%}} \right)^{n-1}}$$ (36)

3

4   In Eq. (36), $\sigma_{0.2\%}$ is the 0.2% proof stress of the material and n is the strain-hardening

5   parameter. For the material under consideration: E_0 = 72.5 GPa, $\sigma_{0.2\%}$ = 534 MPa and n =

6   22, as determined from the provided stress-strain curves in Heimerl and Roy (1945).

7   Iterative calculations are necessary to solve Eq. (34). It is seen from Figure 5 that Eq. (34),

8   representing the flexural buckling load of a perfectly straight column, constitutes an upper

9   bound to the experimental data, which include the effects of initial imperfections.

10

11 **3.2 Pure Torsional Buckling**

12

13 Doubly symmetric sections with low torsional rigidity may be subject to a pure torsional

14 buckling mode. The proposed theory is here verified against experimental data by

15 Hopperstad et al. (1999), who conducted torsional buckling tests on extruded AA6082-T4

16 aluminium cruciform columns. Tests were conducted for five b/t ratios (see Figure 6 for a

17 definition of b and t), while the L/b ratio (with L representing the column length) was kept

18 constant at 6. The out-of-flatness of the flanges was reported to be less than 0.005b. All

19 columns were tested between fixed end plates, so that warping of the end sections was

20 prevented. The boundary conditions for torsion can thus be expressed as:

17

1

2 $\phi = 0$ and $\dfrac{d\phi}{dz} = 0$ for $z = 0,\ z = L$ (37)

3

4 which results in the replacement of Eq. (35) by (Timoshenko and Gere 1961):

5

6 $P_\phi = \dfrac{A}{I_p}\left(G_1 J + E_t C_\omega \dfrac{4\pi^2}{L^2}\right)$ (38)

7

8 The inelastic shear modulus G_1 was calculated using Eq. (21) with $\nu = 0.33$, $\kappa = -0.5$ and

9 with the tangent modulus E_t determined by Eq. (36). The material parameters of the

10 AA6082-T4 alloy, as reported by Hopperstad et al. (1999), are: $E_0 = 69.7$ GPa, $\sigma_{0.2\%} = 131$

11 MPa and $n = 23$. Since the heart lines of the constituent plate elements of the cross-section

12 intersect at the shear centre, the classical theory of torsion (*see* Timoshenko and Gere 1961)

13 dictates that $C_\omega = 0$, leaving only the contribution of pure torsion in Eq. (35):

14

15 $\sigma_{cr} = \dfrac{P_\phi}{A} = \dfrac{G_1 J}{I_p} = G_1 \dfrac{4bt^3/3}{4b^3 t/3} = G_1\left(\dfrac{t}{b}\right)^2$ (39)

16

17 However, a more accurate approach originates from the realization that torsional buckling

18 of the cruciform column is synonymous with local buckling of the four constituent flanges

19 as plates simply supported along one longitudinal edge, with the other longitudinal edge

1 free (Figure 6), and that consequently longitudinal bending stresses develop in the flanges

2 during torsional buckling. These bending stresses implied by plate theory are indeed

3 equivalent to the warping stresses in the context of column theory. This allows for a more

4 accurate determination of C_ω by noting that, if transverse plate bending is neglected (Figure

5 7):

6

7 $$v(x,z) = \phi(z).x \tag{40}$$

8

9 and that the moment per unit plate width M_x is given by:

10

11 $$M_x = E_t \frac{t^3}{12} \frac{d^2 v}{dz^2} = E_t \frac{t^3}{12} \frac{d^2 \phi}{dz^2} x \tag{41}$$

12

13 Consequently, the shear force per unit plate width V_x is given by:

14

15 $$V_x = \frac{dM_x}{dz} = E_t \frac{t^3}{12} \frac{d^3 \phi}{dz^3} x \tag{42}$$

16

17 And the associated torsional moment is:

18

19 $$T_2 = -4 \int_0^b V_x x \, dx = -E_t \frac{b^3 t^3}{9} \frac{d^3 \phi}{dz^3} \tag{43}$$

20

1   which yields:

2

3    $$C_{\omega} = \frac{b^3 t^3}{9}$$ (44)

4

5   A slightly more accurate equation can be obtained by replacing Eq. (41) by the expression

6   for M_x obtained from inelastic plate theory (Becque 2010), while maintaining the

7   displacement field proposed by Eq. (40):

8

9    $$M_x = \frac{t^3}{12} \frac{E_0 E_t}{(1+\nu\kappa)E_0 - \nu(\nu+\kappa)E_t} \left(\frac{\partial^2 v}{\partial z^2} + \nu \frac{\partial^2 v}{\partial x^2} \right) = \frac{t^3}{12} \frac{E_0 E_t}{(1+\nu\kappa)E_0 - \nu(\nu+\kappa)E_t} \frac{d^2 \phi}{dz^2} x$$

10   (45)

11   The corresponding shear force is:

12

13    $$V_x = \frac{\partial M_x}{\partial z} + \frac{\partial M_{yx}}{\partial x},$$ (46)

14

15   where $M_{yx} = 0$ as a result of Eq. (40).

16   Eq. (38) then becomes:

17

18    $$\sigma_{cr} = \frac{P_{\phi}}{A} = G_1 \left(\frac{t}{b} \right)^2 + \frac{E_0 E_t}{(1+\nu\kappa)E_0 - \nu(\nu+\kappa)E_t} \frac{\pi^2}{3} \left(\frac{t}{L} \right)^2$$ (47)

19

1   Since the warping resistance of the cruciform section is a priori small, Eq. (47) leads to

2   predictions which differ by less than 0.5% from the results of Eq. (38), combined with Eq.

3   (44), for the examples here considered.

4   Figure 8 plots the experimental results reported by Hopperstad et al. (1999) and compares

5   them with the predictions of Eq. (38), using Eq. (44) to calculate C_ω. Iterative calculations

6   are again necessary to solve Eq. (38). Good agreement between the predicted and the

7   experimentally measured buckling stresses is obtained: the average ratio of the predicted to

8   the measured buckling stress is 0.98. For comparison, Figure 8 also displays Ilyushin's

9   (1947) solution for the buckling problem of a cruciform column, which is based on plastic

10   deformation theory:

11

12   $$\sigma_{cr} = \frac{E_t}{3}\left[\frac{4\pi^2}{3}\left(\frac{b}{L}\right)^2 + \frac{E_s}{E_t}\left(\frac{t}{b}\right)^2\right] \tag{48}$$

13

14   where E_s is the secant modulus.

15   On a related note, it is seen from the experimental data that, since plates possess significant

16   post-buckling capacity, the ultimate stress of the cruciform columns can considerably

17   outreach the buckling stress. This is particularly true for the longer specimens, which

18   buckle elastically.

19   Figure 9 compares the experimental data of Hopperstad et al. (1999) to two alternate

20   solutions, the first of which was obtained from inelastic plate theory (Becque 2010), while

21   the second one resulted from applying Eq. (39). With respect to Eq. (39), it is noted that the

21

1   omitted term in Eq. (38) becomes smaller for smaller values of E_t (meaning larger stresses

2   and thus smaller b/t values), but on the other hand increases for larger C_ω/L^2 values (which

3   also means smaller b/t values in Fig. 9, since the aspect ratio b/L is fixed). Which effect

4   will dominate depends on the material stress-strain curve. With respect to the solution

5   obtained from inelastic plate theory, each flange is regarded as a plate simply supported

6   along three edges with one longitudinal edge free. Neither theory accounts for the slight

7   rotational end restraint present in the experiments, which becomes relatively more

8   important for longer specimens. On the other hand, for very short columns, plate theory

9   yields better predictions over Eq. (38) because column theory fails to account for the

10   transverse plate bending, which becomes important in shorter specimens.

11

12   **4. COLUMNS WITH A SINGLY SYMMETRIC CROSS-SECTION**

13

14   If the x-axis is an axis of symmetry, then: $y_0 = 0$, and Eqs. (26-28) become:

15

16   $$E_t I_y \frac{d^2 u}{dz^2} + Pu = 0 \tag{49}$$

17

18   $$E_t I_x \frac{d^2 v}{dz^2} + P(v - x_0 \phi) = 0 \tag{50}$$

19

20   $$E_t C_\omega \frac{d^4 \phi}{dz^4} - \left(G_1 J - \frac{I_p}{A} P\right) \frac{d^2 \phi}{dz^2} - P x_0 \frac{d^2 v}{dz^2} = 0 \tag{51}$$

1

2   The flexural buckling mode about the y-axis, described by Eq. (49), which is dependent on

3   u, is uncoupled from the flexural-torsional buckling mode in the y-direction, described by

4   Eqs. (50-51), which contain v and ϕ. If the column ends are free to rotate about the x- and

5   y-axes, but prevented from warping and rotating about the longitudinal axis, the flexural-

6   torsional buckling load P is determined by the equation (*see* Timoshenko and Gere 1961):

7

8   $$\frac{I_x + I_y}{I_p} P^2 - (P_x + P_\phi)P + P_x P_\phi = 0 \qquad (52)$$

9

10 where P_x and P_ϕ are given by Eqs. (33) and (38) respectively. Consequently:

11

12 $$P = \frac{I_p}{2(I_x + I_y)}\left[P_x + P_\phi - \sqrt{(P_x + P_\phi)^2 - 4P_x P_\phi \frac{I_x + I_y}{I_p}}\right] \qquad (53)$$

13

14 Eq. (53) is first verified against experimental data provided by Leary and Holt (1946). The

15 researchers tested equal-leg angles with dimensions 63.5mm x 63.5mm x 6.35mm,

16 manufactured by extrusion of 14S-T aluminium. The reported material properties are: $E_0 =$

17 73.1 GPa, $\sigma_{0.2\%} = 394$ MPa, n = 27 and $v = 0.33$. The overall imperfections were reported to

18 be less than L/1000. Using Eq. (44), the warping constant C_ω was calculated as:

19

1 $$C_\omega = \frac{b^3 t^3}{18}$$ (54)

2

3 Figure 10 compares the experimental data to the theoretical predictions. Iterative

4 calculations are necessary to solve Eq. (53). The theory confirms the experimental

5 observation that the longer columns fail by flexural buckling about the weak principal axis

6 of the angle, while the shorter columns fail by flexural-torsional buckling. A close match

7 between the theory and the experiment is obtained, with an average ratio of the predicted to

8 the measured load of 1.00 for the specimens failing by flexural-torsional buckling. It should

9 be noted that the test data represent ultimate (failure) stresses, while the theory predicts

10 buckling stresses. The close match suggests that post-buckling capacity is limited for this

11 type of inelastic buckling.

12 Secondly, Eq. (53) is verified against tests on 3Cr12 stainless steel hat section columns,

13 failing by flexural-torsional buckling (van den Berg 1988). The material properties, as

14 reported by van den Berg are: E_0 = 222 GPa, $\sigma_{0.2\%}$ = 319 MPa and n = 6.3. The cross-

15 sectional dimensions are shown in Fig. 11. Figure 12 compares the results of Eq. (53) with

16 the experimental data in dashed line. It is seen that the capacity of the shorter specimens

17 significantly exceeds the predictions. The difference can be attributed to the fact that the

18 sections were cold-formed, resulting in significantly increased corner properties (*see*,

19 among others, Lecce 2006, Becque 2009). Due to the location of the corners with respect to

20 the principal axes, the enhanced corner areas considerably increase the effective second

21 moment of area I_y, while also improving the warping resistance. This effect becomes more

1   pronounced for specimens failing at higher stresses in the inelastic range. To take into

2   account these enhanced corner properties, the cross-sectional properties I_x, I_y, A, J and C_ω

3   were recalculated, where the corners were given an equivalent increased thickness t_{eq}:

4

5    $$t_{eq} = \frac{E_{tc}}{E_t} t \qquad\qquad\qquad (55)$$

6

7   In the above Eq. (53), E_t is the tangent modulus of the material constituting the flat

8   segments of the cross-section, while E_{tc} is the tangent modulus of the rounded corner

9   material, calculated at the same strain value. The Ramberg-Osgood parameters necessary to

10   calculate E_{tc} were obtained from Lecce (2006): $\sigma_{0.2\%} = 571$ MPa and n = 4. Iterative

11   calculations are necessary to ensure E_t is calculated at the buckling stress. Figure 12

12   displays the results of these calculations in solid line. The inelastic local buckling stress of

13   the cross-section, which was calculated using the method set out by Becque et al. (2011), is

14   also indicated. It is seen that good agreement is obtained between the predictions of Eq.

15   (53), taking into account the enhanced corners, and the experimental data, up to a stress

16   level slightly below the inelastic local buckling load. Above this level, local-overall

17   interaction buckling becomes the governing failure mode, which cannot be accounted for

18   using this column theory. The average ration of predicted to experimental load is 1.00 for

19   the specimens failing in pure flexural-torsional buckling.

20

21   **CONCLUSIONS**

1

2 The paper presents the differential equations governing flexural, torsional and flexural-

3 torsional buckling of inelastic columns. The theory is consistent with the principles of

4 plastic flow theory and avoids the plastic buckling paradox by deriving an expression for

5 the inelastic shear stiffness while considering an infinitesimal solid element transitioning to

6 its shear-deformed state.

7 The theory is verified against experimental data available in literature, including examples

8 of the pure flexural and pure torsional buckling modes of columns with a doubly symmetric

9 cross-section, as well as examples of the flexural and flexural-torsional buckling modes of

10 columns with a singly symmetric cross-section. Good agreement between the theory and

11 the experiment is observed over the whole range of buckling modes.

12

13

1 **REFERENCES**

2

3 Batdorf, S.B. (1949). "Theories of Plastic Buckling." *Journal of the Aeronautical Sciences*, July,

4   404-408.

5

6 Bazant, Z.P., and Cedolin, L. (1991). *Stability of Structures*, Oxford University Press, Oxford, U.K.

7

8 Becque, J. (2009). "Experimental Investigation of Local-Overall Interaction Buckling of Stainless

9   Steel Lipped Channel Columns." *Journal of Constructional Steel Research*, 65, 1677-1684.

10

11 Becque, J. (2010). "Inelastic Plate Buckling" *Journal of Engineering Mechanics*, ASCE, 136(9),

12   1123-1130.

13

14 Becque, J., Lathourakis, P., and Jones, R. (2011). "Experimental verification of an inelastic plate

15   theory based on plastic flow theory." *Thin-Walled Structures*, 49(12), 1563-1572.

16

17 Bleich, H., and Bleich, F. (1936). "Biegung, Drillung und Knickung von Stäben aus Dünnen

18   Wänden." Vorbericht zum 2. Kongress der Internazionalen Vereinigung für Brücken- und

19   Hochbau. Verlag Ernst & Sohn, Berlin.

20

21 Considère, A. (1891). "Resistance des pièces comprimées." Congrès international des procédés de

22   construction, Paris, Vol. 3, p. 371.

23

1   Drucker, D.C. (1950). "Some Implications of Work Hardening and Ideal Plasticity." *Quarterly of*

2   *Applied Mathematics* 7, p. 411-418.

3

4   Engesser, F. (1889). *Zeitschrift fur Architektur und Ingenieurwesen,* 35, 455.

5

6   Engesser, F. (1895). *Schweizerische Bauzeitung,* 26, 24.

7

8   Gonçalves, R., and Camotim, D. (2007). "Thin-walled member plastic bifurcation analysis using

9   generalised beam theory." *Advances in Engineering Software*, 38, pp. 637-646.

10

11   Goodier, J.N. (1942). "Flexural-Torsional Buckling of Bars of Open Section." *Cornell University*

12   *Engineering Experiment Station Bulletin*, 28, 16p.

13

14   Heimerl, G.J., and Roy, J.A. (1945). "Column and Plate Compressive Strengths of Aircraft

15   Structural Materials – Extruded 75S-T Aluminum Alloy" *NACA Wartime Report*, originally

16   issued as Advance Restricted Report L5F08a.

17

18   Holt, M., and Leary, J.R. (1946). "The Column Strength of Aluminum Alloy 75S-T Extruded

19   Shapes." *NACA Technical Note No. 1004*.

20

21   Hopperstad, O.S., Langseth, M., and Tryland, T. (1999). "Ultimate Strength of Aluminium Alloy

22   Outstands in Compression: Experiments and Simplified Analysis." *Thin-Walled Structures*,

23   34, 279-294.

24

1   Hutchinson, J.W. (1974). "Plastic Buckling." *Advances in Applied Mechanics*, C-S. Yih, ed.,

2   Academic, New York, 67-144.

3

4   Hutchinson, J.W., and Budiansky, B. (1976). "Analytical and Numerical Study of the Effects of

5   Initial Imperfections on the Inelastic Buckling of a Cruciform Column." *Buckling of*

6   *Structures, Proceedings of the IUTAM Symposium, Cambridge, Massachussets*, B.

7   Budiansky, editor, Springer, Berlin, 98-105.

8

9   Ilyushin, A.A. (1947). "The Elasto-Plastic Stability of Plates." *NACA Technical Note No. 1188.*

10

11   Johnson, A., and Winter, G.. (1966). "Behaviour of Stainless Steel Columns and Beams." *Journal*

12   *of Structural Engineering, American Society of Civil Engineers, ASCE* 92(ST5), 97-118.

13

14   Kappus, R. (1937) "Drillknicken zentrisch gedruckter Stabe mit offenem Profil im elastischen

15   Bereich." *Luftfahrtforschung*, 14 (9), 444-457 (translated into *NACA Technical*

16   *Memorandum No. 851* (1938)).

17

18   Leary, J.R., and Holt, M. (1946). "Column Strength of Aluminum Alloy 14S-T Extruded Shapes

19   and Rod." *NACA Technical Note No. 1027*.

20

21   Lecce, M. (2006). *Distortional Buckling of Stainless Steel Sections.* PhD Thesis, School of Civil

22   Engineering, University of Sydney, Sydney.

23

24   Lubliner, J. (1990). *Plasticity Theory*, Macmillan, New York.

1

2 Onat, E.T., and Drucker, D.C. (1953). "Inelastic Instability and Incremental Theories of Plasticity."

3   *Journal of the Aeronautical Sciences*, 20(3), 181-186.

4

5 Osgood, W.R., and Holt, M. (1938). "The Column Strength of Two Extruded Aluminum-Alloy H-

6   Sections." *NACA Technical Report No. 656*.

7

8 Ramberg, W., and Osgood, W.R. (1943). *NACA Technical Note No. 902*.

9

10 Rasmussen, K.J.R., and Hancock, G.J. (1993). "Design of Cold-Formed Stainless Steel Tubular

11   Members. I: Columns." *Journal of Structural Engineering*, 119(8), 2349-2367.

12

13 Rønning, L., Hopperstad, O.S., and Larsen, P.K. (2010). "Numerical study of the effects of

14   constitutive models on plastic buckling of plate elements." *European Journal of*

15   *Mechanics A/Solids*, 29, pp. 508-522.

16

17 Ruocco, E. (2015). "Elastoplastic buckling analysis of thin-walled structures." *Aerospace*

18   *Science and Technology*, 43, pp. 176-190.

19

20 Shamass, R., Alfano, G., and Guarracino, F. (2015). "An investigation into the plastic buckling

21   paradox for circular cylindrical shells under non-proportional loading." *Thin-Walled*

22   *Structures*, 95, pp. 347-362.

23

1 Shanley, F. (1947). "Inelastic Column Theory." *Journal of the Aeronautical Sciences*, 14(5), 261-

2   276.

3

4 Timoshenko, S.P. (1945). "Theory of Bending, Torsion and Buckling of Thin-Walled Members of

5   Open Cross-Section." *Journal of the Franklin Institute*, 239(5), 343-361.

6

7 Timoshenko, S.P., and Gere, J.M. (1961). *Theory of Elastic Stability*, 2nd edition, McGraw-Hill,

8   New York.

9

10 van den Berg, G.J. (1988). "The Torsional-Flexural Buckling Strength of Cold-Formed Stainless

11   Steel Columns." *Proceedings of the Ninth International Specialty Conference on Cold-

12   Formed Steel Structures*, Missouri-Rolla, eds. Yu, W.W., and Senne, J.H.

13

14 van den Berg, G.J. (2000). "The Effect of the Non-Linear Stress-Strain Behaviour of Stainless Steel

15   on Member Capacity." *Journal of Constructional Steel Research*, 54(1), 135-160.

16

17 Wagner, H., and Pretschner, W. (1936). *Luftfahrtforschung*, 11, 174-180 (translated into *NACA*

18   *Technical Memorandum No. 784*).

19

20 Wang, C.M., and Tun Myint Aung (2007). "Plastic buckling analysis of thick plates using p-Ritz

21   method" *International Journal of Solids and Structures*, 44, 6239-6255.

22

23 Wang, C.M., Xiang, Y., and Chakrabarty, J. (2001). "Elastic/plastic buckling of thick plates."

24   *International Journal of Solids and Structures*, 38, 8617-8640.

1

2   Wang, X., and Huang, J. (2009). "Elastoplastic buckling analyses of rectangular plates under biaxial

3   loadings by the differential quadrature method." *Thin-Walled Structures*, 47, 14-20.

4
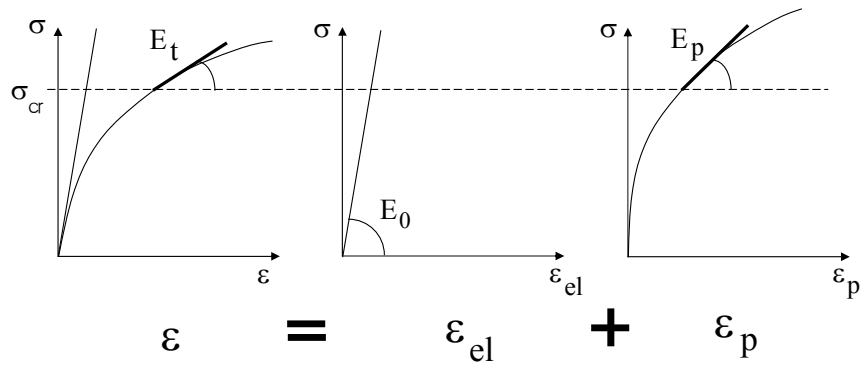
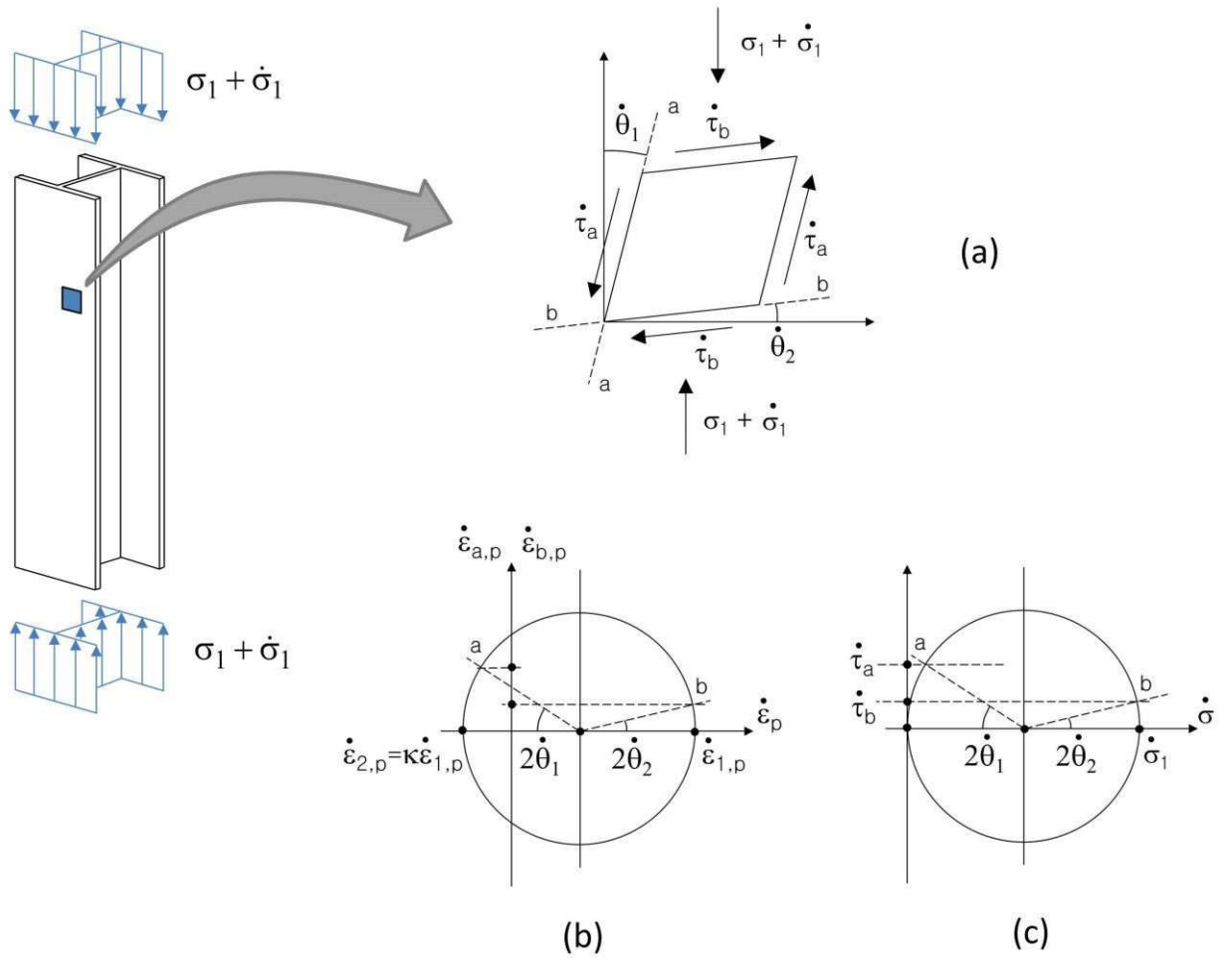**Figure 1. Material stress-strain curve**
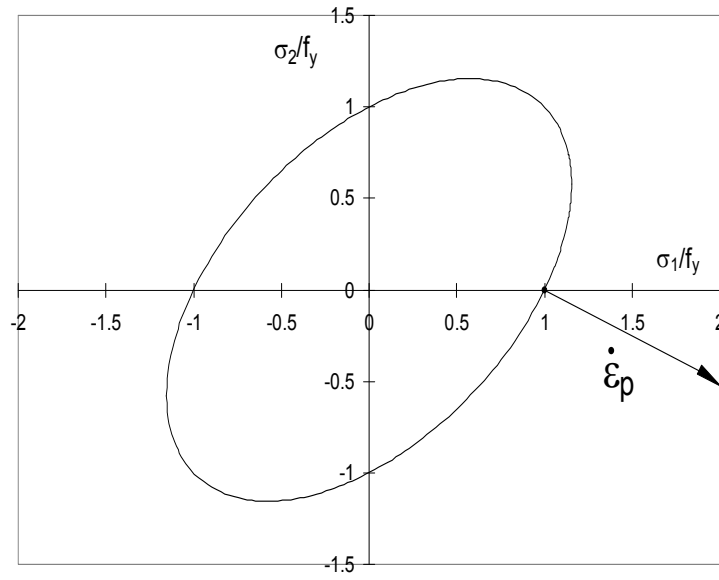
Figure 2. von Mises surface

Figure 3. a. Infinitesimal element within the column, b. Mohr's circle of incremental plastic strain, c. Mohr's circle of incremental stress
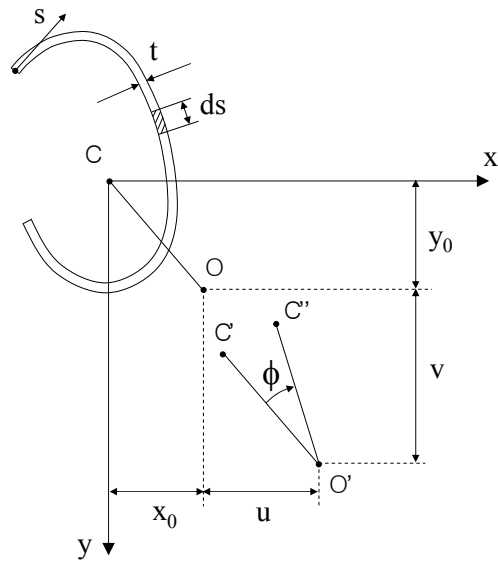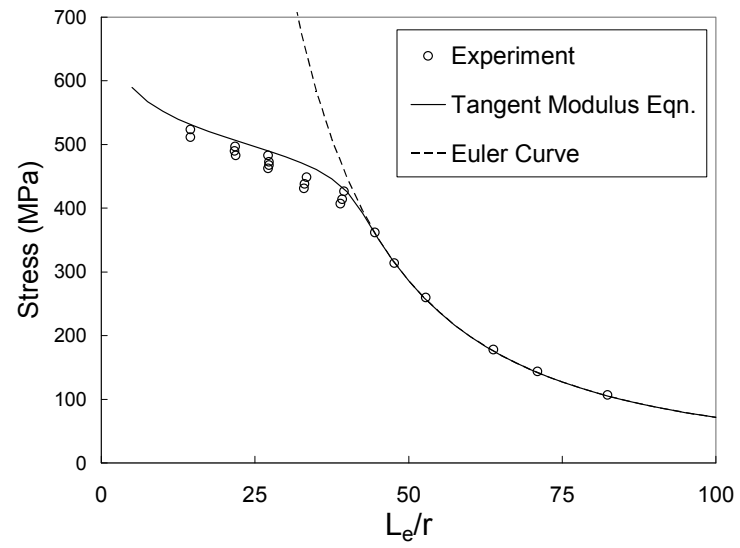
Figure 4. Column cross-section

Figure 5. Tangent modulus curve vs. flexural buckling stress
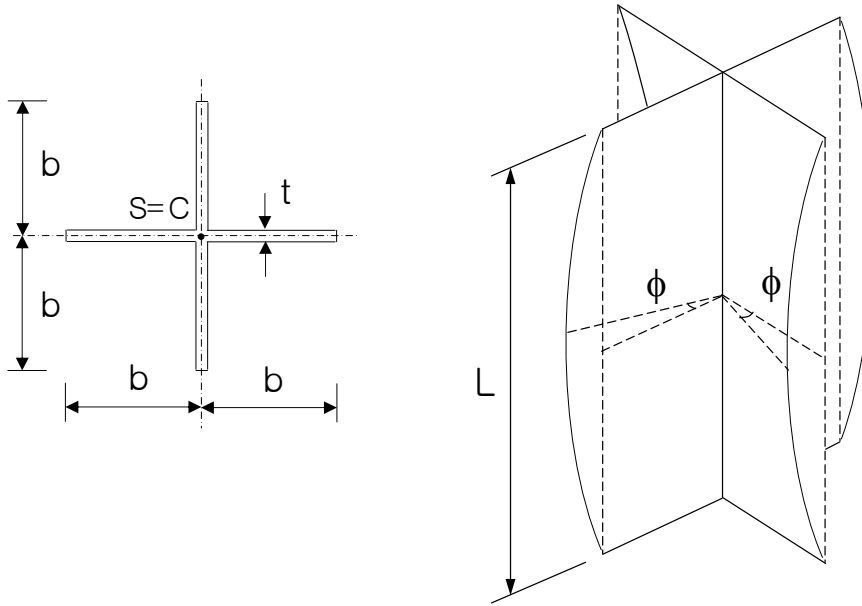
Figure 6. Torsional buckling of a cruciform column
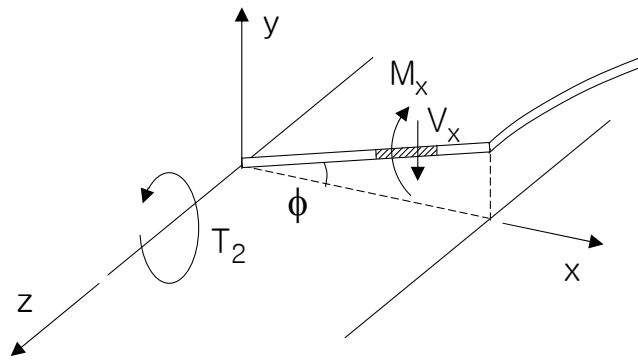
Figure 7. Flange in deformed state
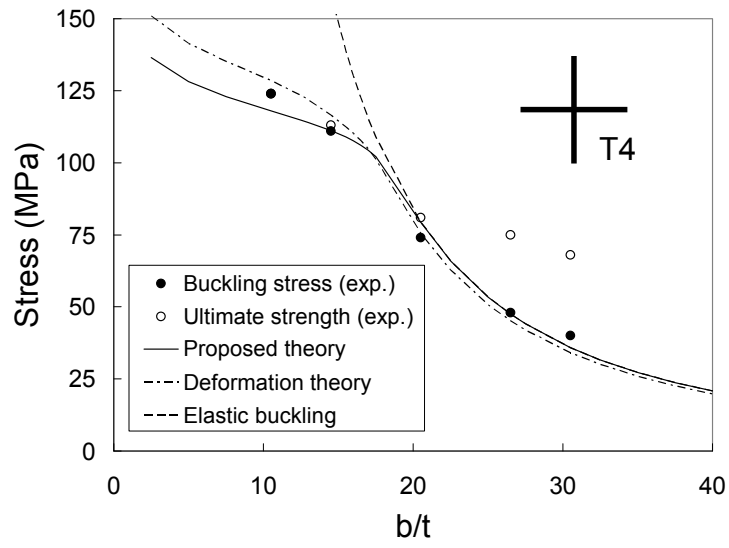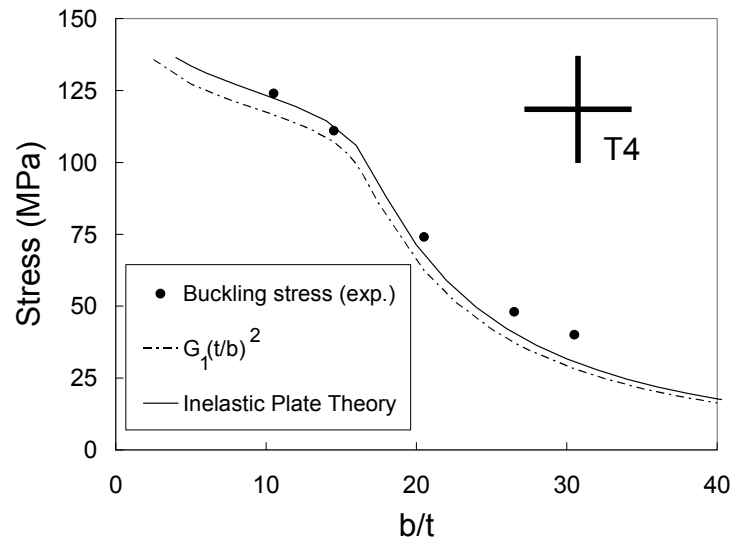
Figure 8. Torsional buckling of a cruciform section (AA6082-T4)
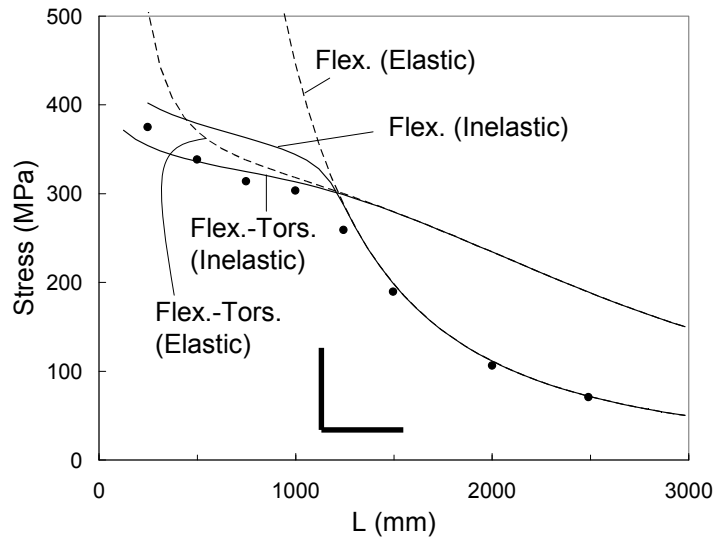
Figure 9. Approximate solutions for the cruciform column buckling problem

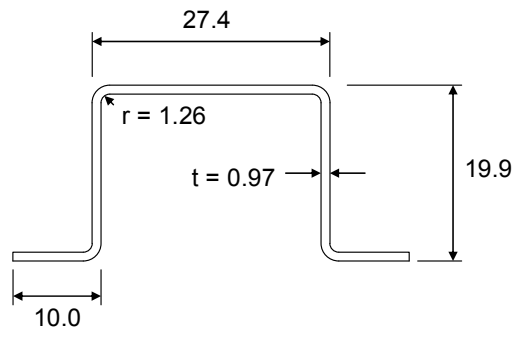**Figure 10. Flexural-torsional buckling of aluminium angles**
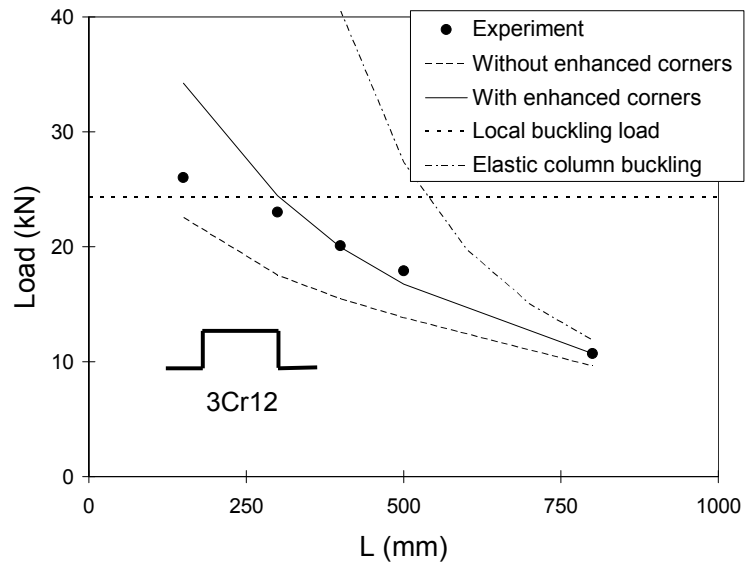
Figure 11. Hat section dimensions (in mm)

Figure 12. Flexural-torsional buckling of a hat section column